Automotive Science and Engineering, Vol. 12, No. 2, (2022), 3838-3846

Iran University of Science and Technology

Automotive science and Engineering

Journal Homepage: ase.iust.ac.ir

ISSN: 2008-9899

Machine Vision–Based Measurement Approach for Engine Accessory Belt Transverse Vibration Based on Deep Learning Method

Ashkan Moosavian[1*], Alireza Hosseini[2], Seyed Mohammad Jafari[3], Iman Chitsaz[4], Shahriar Baradaran Shokouhi[2]

[1]Department of Agricultural Engineering, Technical and Vocational University (TVU), Tehran, Iran

[2]School of Electrical Engineering, Iran University of Science and Technology (IUST), Tehran, Iran

[3]Faculty of Mechanical & Energy Engineering, Shahid Beheshti University, A.C., Tehran, Iran

[4]Department of Mechanical Engineering, Isfahan University of Technology, Isfahan, 84156-83111, Iran

ARTICLE INFO

Article history:
Received: 16 May 2022
Accepted: 13 Jun 2022
Published: 13 Jun 2022

Keywords:
IC engine
Accessory belt
Mask-RCNN
Semantic segmentation
Machine vision

A B S T R A C T

In this paper, to address the problem of using displacement sensors in measuring the transverse vibration of engine accessory belt, a novel non-contact method based on machine vision and Mask-RCNN model is proposed. Mask-RCNN model was trained using the videos captured by a high speed camera. The results showed that RCNN model had an accuracy of 93% in detection of the accessory belt during the test. Afterward, the belt curve was obtained by a polynomial regression to obtain its performance parameters. The results showed that normal vibration of the center of the belt was in the range of 2 to 3 mm, but the maximum vibration was 8.7 mm and happened in the engine speed of 4200 rpm. Also, vibration frequency of the belt was obtained 124 Hz. Moreover, the minimum belt oscillation occurred at the beginning point of the belt on the TVD pulley, whereas the maximum oscillation occurred at a point close to the center of the belt at a distance of 16 mm from it. The results show that the proposed method can effectively be used for determination of the transvers vibration of the engine accessory belts, because despite the precise measurement of the belt vibration at any point, can provide the instantaneous position curve of all belt points and the equation of the belt curve at any moment. Useful information such as the belt point having the maximum vibration, belt slope, vibration frequency and scatter band of the belt vibration can be obtained as well.

*Corresponding Author
Email Address: a_moosavian@tvu.ac.ir
https://doi.org/10.22068/ase.2022.611

[DOI: 10.22068/ase.2022.611]

1. Introduction

The performance of some vehicle equipment such as lighting, air conditioning and power consumption depends on the performance of the engine accessories system, especially accessory belt. To ensure the health and performance of the belt in terms of the amount of vibrations, durability, slippage, etc, validation tests at different speeds and temperatures are designed and applied to engine accessory belt. These tests are divided into two groups of functional and durability tests. One of the important validation tests for the accessory belt, is flapping test. This test includes a speed sweep from idle to maximum speed of the engine during a little time [1]. When the belt resonates, large oscillations occurred on it. Those speeds in which the belt experiences its most severe oscillations are called critical or resonant speeds of the belt. The main purpose of performing the belt flapping test is to find these critical speeds because the belt failures occur in these speeds, since the belt will have the most fluctuations and consequently the largest stresses in the critical speeds, so this is the worst case for belt operation [1]. After obtaining the critical speeds, the durability tests of the belt are designed and performed at these speeds. If the belt does not show any failure sign after the durability test, it is concluded that the belt has enough useful life.

One of the most essential aspects of the belt flapping test is measuring the belt transverse vibrations in order to identify the critical speed of the belt. Traditionally in engine testing laboratories, the measurement of transverse vibration is performed based on displacement sensors such as Laser Doppler Vibrometer (LDV) [2-4], proximity sensors [5] and electrostatic sensors [6]. In sensor-based method such as LDV, the sensor is first mounted on the engine through a fixture where the maximum free length of the belt is located. Then, by shining a laser beam on the belt strip, the belt oscillation during its operation is measured in the form of a time-domain signal. Many researchers have used this method so far, for example, Ucar et al [7] designed a fault detection system for automotive timing belts based on displacement sensor method. They used three optical sensors in the experiments. Hu et al [8] developed an electrostatic sensing-based measurement method for non-contact monitoring of belt vibration. In this research, it was mentioned that the measurement of transverse vibration in a moving belt is a difficult task. Also, a good comparison was made between the different experimental methods for belt vibration measurement. Khazaee et al [9] proposed an intelligent method for life prediction of timing belt of an internal combustion (IC) engine using vibration analysis and neural network model. They used LDV method to obtain vibration signals of the belt.

Belt vibration measurement based on displacement sensors has major drawbacks; these sensors lose their accuracy over time. Also, because the sensors must be installed on the engine body, they need some preparing processes such as drilling, making fixtures, installation, etc. Another disadvantage of installing the sensors on the engine is the damages that may occur on the sensors in the long operating time due to permanent and severe fluctuations of the engine caused by stimulation of various components inside and outside the engine. Moreover, such instruments may be excessively expensive to perform in routine industrial applications.

Due to the mentioned shortcomings, in order to update the engine validation tests that are required by all engine manufacturers today, it is necessary to develop a method for measuring belt vibrations that firstly does not require preparation and installation processes on the engine, and secondly to be accurate, fast, and without loss function over time.

Nowadays, the use of machine vision methods with combination of artificial intelligence has many applications such as in automotive [10], agriculture [11] and robotics [12]. Among the artificial intelligence methods, deep learning techniques has attracted lots of attentions because of its high capabilities in solving various nonlinear complex problems [13, 14]. Currently, the machine vision systems equipped with artificial intelligence have provided practical solutions for IC engines relevant issues. In this regard, Ramamoorthy [15] developed a machine vision-based method for evaluating

[DOI: 10.22068/ase.2022.611]

honing angle of cylinder liners based on cylinder liner images. In another research, Lawrence et al [16] used a machine vision approach to characterize cylinder bore surface topography. They could estimate Abbott-Firestone curve parameters by processing the images of the cylinder liner surface and using ANN method. Xuyun et al [17] presented a novel fault detection system for aircraft engines based on machine vision approach and convolutional neural network (CNN). Capela et al [18] proposed an inspection machine vision-based system to detect the engine labels using Faster-RCNN and YOLOv3 object detection methods. Rochussen and Kirchen [19] presented a robust image segmentation algorithm for feature extraction from single-cycle in-cylinder combustion images.

Based on the above descriptions, to overcome the shortcomings of the traditional belt vibration measurement methods, the current paper as a new work, presents an efficient method based on machine vision and deep learning method to obtain the transverse vibrations of the belt, which has not been studied in the previous studies. This method, firstly, does not have the disadvantages of the traditional displacement sensor method. Secondly, it can provide more capabilities for the measurement. Thirdly, it has the potential for multiple applications, meaning that other applications such as fault detection of belt and other accessory parts, can be set up beside the measurement of the belt vibrations at the same time. The present method comprises of some analysis stage which is shown in Figure 1.

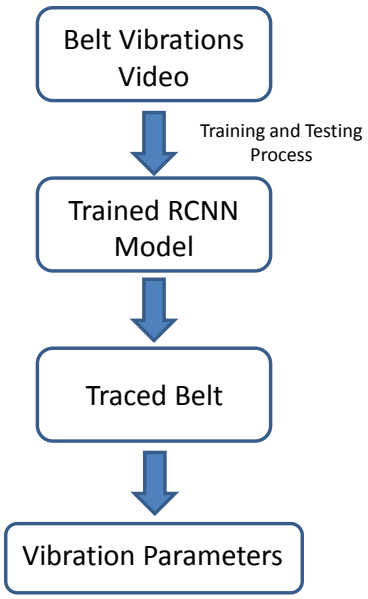

Figure 1: Flowchart of the present work

2. Materials and Methods

2.1. Experimental Setup

The experiments were implemented on an inline four-cylinder gasoline engine. Table 1 shows the engine specifications. In order to control the engine speed and load, the engine was coupled with a 190 kW eddy-current dynamometer. Different engine parameters such as speed and torque, oil temperature and pressure, water temperature and pressure, ambient temperature and pressure, throttle position and exhaust manifold temperature were measured during the tests.

Table 1: Engine specifications

Engine type	Gasoline 4-cylinder inline
Bore × Stroke (mm)	78 × 85
Volume (L)	1.650
Compression ratio	11.5
Max. Power (kW @ rpm)	83 @ 6000
Max. Torque (Nm @ rpm)	146 @ 3500-4500

In this study, adopted from the belt flapping test procedure designed by PSA Peugeot Citroën [20], the engine speed was swept from the idle speed to maximum speed i.e. 6000 rpm under full load condition during about 25 seconds. Simultaneously, the video of the belt oscillations was captured using a high-speed camera model Casio Exilim EX-F1 with a rate of 1200 frames per second (fps). Fig. 2 shows the experimental test setup. Note that the experiment was repeated four times to observe reproducibility.

The camera was set to capture the frame of the free length of the belt between the air compressor (AC) compressor pulley and torsional vibration damper (TVD) pulley, because this distance has the longest in the timing system so the maximum belt oscillations occur here, meaning that this area is the worst case for the belt oscillations.

[DOI: 10.22068/ase.2022.611]

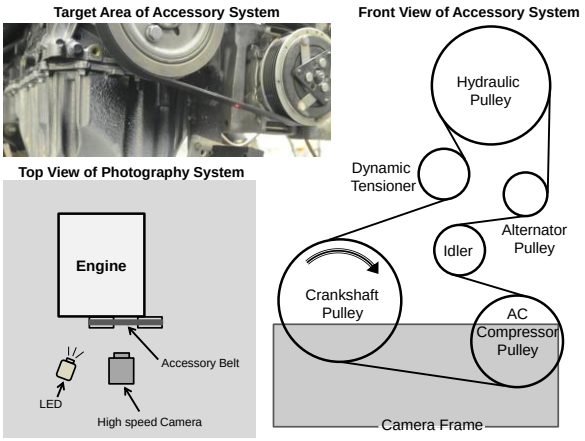

Figure 2: The experimental setup

2.2. Deep Learning Method

Deep Learning is a branch of machine learning which applies algorithms inspired by the structure of the human brain. Deep learning lets computational models learn and demonstrate data with several levels of abstraction mimicking, consequently it implicitly catches complex structures of large-scale data [21]. Using Convolutional Neural Networks (CNNs), the explicit extraction of information from visual data is possible [22]. A CNN includes three different layers namely, pooling, convolutional and fully connected layers each one playing a specific role. CNN has extremely been successful in computer vision applications. A developed version of CNN is the Region Proposal Convolutional Neural Network algorithm (or R-CNN) [23]. In R-CNN, an image is split into several areas and is separately processed. The first RCNN version split the image into a large number of regions according to a selective search algorithm, and then it was fed to CNN. The great results could be obtained by this procedure, but the time consumed to train the model was huge indeed. Therefore, this method is not practical for real-time problems. The RCNN technique was further refined. Instead of feeding the model with a large number of separate images, the initial input image is received in order to calculate its feature map and then choose the regions of interest [18]. Due to the time needed to train the algorithm and to identify and categorize the objects, a faster version was developed namely Fast R-CNN24. Fast R-CNN gives a quicker training process but it is not proper for real-time applications. In Faster R-CNN [25], the areas of interest that are fed to the network, are predicted and reshaped using a separated CNN. Faster R-CNN is more appropriate for real-time detection, because of little time needed to implement the recognition on an image as well as obtaining the high accuracy [26].

Deep neural networks are properly capable of semantic segmentation, which plays a significant role in image understanding and analysis. An extension version of Faster-RCNN, namely Mask R-CNN [27] is the most advanced tool for image segmentation, in which the pixels of each object are located instead of the bounding boxes [18]. This version of network identifies objects of the image, and makes a high-quality segmentation mask for each case. Mask R-CNN was constructed by Faster R-CNN. Faster R-CNN has two outputs for each desired object, class label and bounding box offset, but Mask R-CNN is the addition of a third part that outputs the object mask. The extra mask output is different from the class and box outputs, needing the extraction of a much better spatial layout of an object.

In this research, a Mask-RCNN with the configuration shown in Table 2, were used to segment the accessory belt from the other parts. Each frame of the videos from the belt vibrations was given to the designed network. The output of this network was the coordinates of all the pixels including the belt in the image.

Table 2: Configuration of designed Mask-RCNN

Backbone	Resnet101
Backbone Strides	[4,8,16,32,64]
Learning Momentum	0.9
Learning Rate	0.001
Mask Pool Size	14
Number of Epochs	300
Steps per Epoch	10
Pool Size	7
Loss Function	0.07

[DOI: 10.22068/ase.2022.611]

3. Results and Discussion

After recording the videos from the belt oscillations, all videos were divided into their frames. Some samples of these frames are shown in Figure 3.

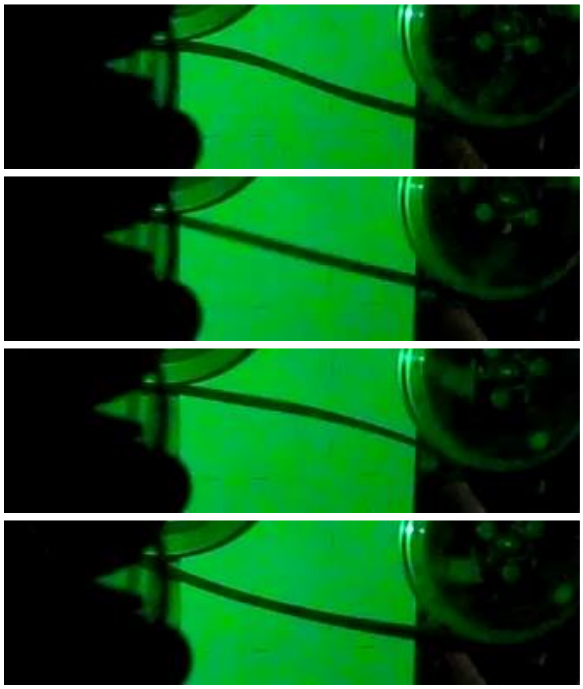

Figure 3: Samples of the belt oscillation captured by the high speed camera

At next stage, Mask-RCNN model was trained and then tested. As mentioned before, the video capturing process during the flapping test was repeated four times, meaning that four videos were gained from the belt oscillations during the experiments. In the training stage, 110 frames from the first video were fed to Mask-RCNN model as training data. To make the labeled data, the manual segmentation method was used to separate the belt from the rest of areas in image. Afterward, the validation and testing processes were implemented on the second and third videos with 40 and 50 frames, respectively. The results showed that the belt was detected in all frames with a high accuracy of 93%. Fig. 4 shows two output samples of the trained Mask-RCNN model. As it can be seen, the belt could be distinguished from the rest of parts in the images, so the trained Mask-RCNN model had suitable capability in detecting the belt. After training and testing the Mask-RCNN model and obtaining the detection accuracy, the trained model was applied on the fourth video to achieve the analysis results.

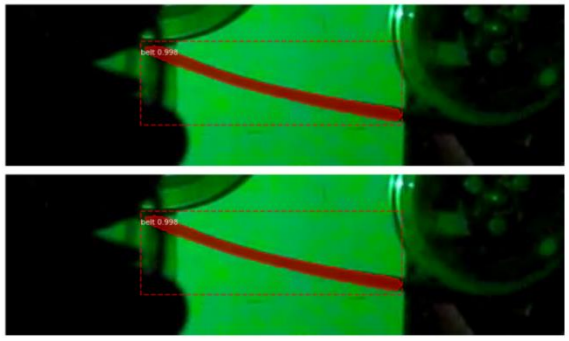

Figure 4: Two random examples of belt detection by the trained Mask-RCNN model

After that, all pixels of the detected belt were separated from the rest of parts in the image. Thus, each frame of the video was converted to a binary image in which the entire image was white and only the pixels of the belt were red. After separating the belt, the curve of the belt central axis and its equation were obtained using the polynomial curve fitting regression interpolation method [28, 29].

Fig. 5 illustrates the step-by-step analysis results for a sample frame of the video taken from the belt oscillation.

Based on the belt shape, its curve was estimated with a 5th degree function. Accordingly, the following equation was obtained for the belt curve shown in Figure 5(d):

$$y = -2.678 \times 10^{-10}x^5 + 3.064 \times 10^{-7}x^4 - 0.0001x^3 + 0.017x^2 - 1.095x + 49.575 \quad (1)$$

where x is in the range of 100 to 240 equal to the position of the beginning and end point of the belt in the original raw image, respectively.

[DOI: 10.22068/ase.2022.611]

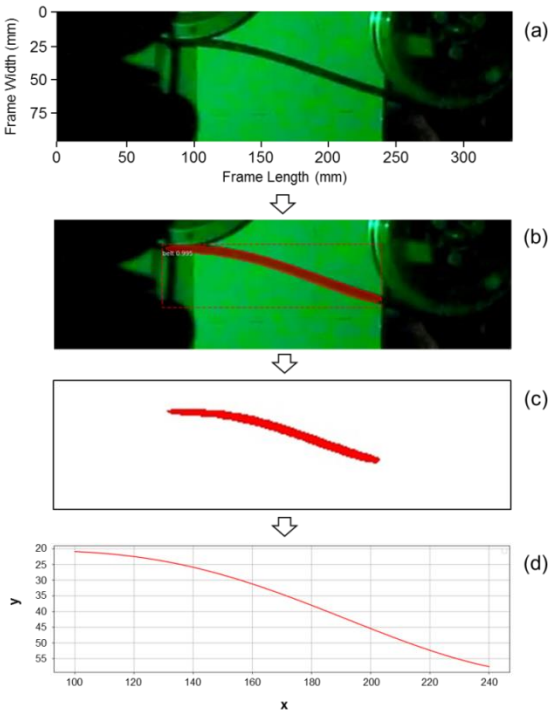

Figure 5: Steps of analysis results: (a) original frame (b) detected belt (c) detached belt in binary image (d) belt curve

Having the equation of the belt curves in each frame, the position of any desired point on the belt during the oscillation can quantitatively be determined. The extremum points of the belt during flapping, the slope of the belt and other parameters of the belt curve are also achievable by this equation. The analysis shown in Fig. 5 was performed for each frame, and the equation of the belt curve was obtained for all frames of the total test duration.

In the next step, to observe the changes in the belt vibration during the whole test, the oscillations of the midpoint of the belt, as an example, were calculated based on the above analysis process for all frames of the video. Fig. 6 shows the belt center oscillations during the entire test.

As can be seen, the normal vibration of the belt was about 2 mm, but the belt experienced severe oscillations at time intervals of about 4 to 8 seconds and 16 to 21 seconds. These two time intervals were equivalent to the engine speeds of about 2500 and 4200 rpm. The maximum vibration occurred approximately at 19th second with the amplitude of 8.7 mm. In this time, the engine speed was 4200 rpm. According to these results, it can be concluded that the speeds of 2500 and 4200 rpm were the critical speed of this belt. The critical speeds are among the main belt characteristics which are used for evaluating its durability [20]. Therefore, finding the critical speeds of the belt was one of the main purposes of the belt flapping test which was well done by the proposed intelligent system.

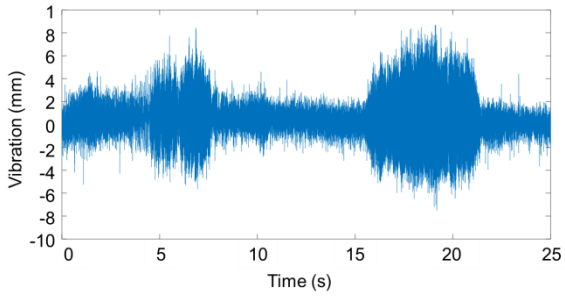

Figure 6: Transverse vibration of the belt center during the flapping test

One of the important functional and durability parameters of the belt which can be obtained from the proposed machine vision system is the oscillation frequency, which depends on the geometric design, materials and dynamic characteristics of the belt. The frequency of the oscillation can be calculated by transferring the time domain vibration signal into the frequency domain. To this end, the frequency spectrum of the belt vibrations is firstly obtained by FFT method. In the obtained spectrum, the dominant frequency indicates the frequency of the belt oscillation. For example, Fig. 7 shows the frequency spectrum of the belt vibration shown in Fig. 6. As it can be seen in this spectrum, the dominant frequency is 124 Hz, so the belt oscillation frequency is 124 Hz i.e. the belt oscillates 124 times per second.

In the last stage, the envelope curve of the belt vibrations was obtained in order to find the range of the space occupied by the belt during its oscillation. To this end, the belt shape curves for each frame were plotted together in a diagram. By this work, the scatter band of the belt vibrations and its maximum and minimum

[DOI: 10.22068/ase.2022.611]

ranges, in other words the borders of the belt vibrations could be observed and calculated. Fig. 8 shows the envelope diagram of the belt vibrations. Samples of the use of this diagram is to compare the performance of different belts, observing the effects of different belt materials and designs on the oscillation, belt failure analysis, help to optimally design the belt and the position of the pulleys, etc. According to the envelope diagram of the belt oscillations, it was found that in this belt, the smallest vibration occurred at the starting point of the belt on TVD pulley with an amplitude of about 7.9 mm, and the largest amplitude belonged to the horizontal position of 154 mm, meaning 16 mm behind the center of the belt, with a magnitude of 16.5 mm.

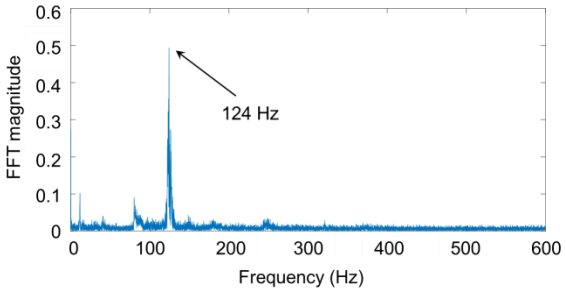

Figure 7: Frequency spectrum of the belt vibration shown in Figure 6

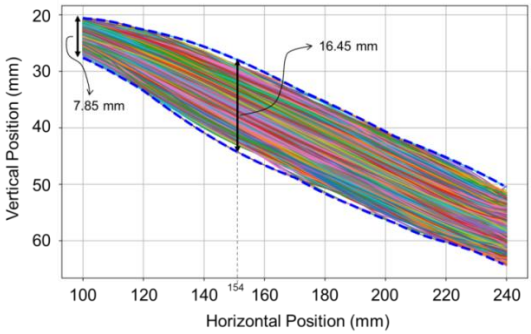

Figure 8: Belt shape curves during the entire test and their envelope

One of the advantages of the proposed intelligent machine vision system despite its high accuracy is that it can be used to obtain the transverse vibrations of any desired point of the belt, whereas in the traditional experimental methods, the vibration of only one limited area of the belt can be measured by laser displacement sensors, so there won't be information about the vibration of the rest of parts of the belt. Moreover, it can be possible to add some more features to this machine vision system in future such as belt fault prediction and determination of the belt linear velocity and tensioner movement pattern. In other words, the proposed system has potential to become a multi-functional system. In overall, the results show the high capabilities of the proposed intelligent method which can effectively be used in the novel validation tests of engine belts like timing and accessory belts.

4. Conclusion

In this paper, an intelligent method was presented to trace the movement of the engine accessory belt and obtain its transverse vibration. To this end, a belt flapping test was designed and performed on a gasoline engine. Simultaneously, the movement of the belt was captured during the entire test using a high speed camera with 1200 fps rate. By a trained Mask-RCNN model, the belt strip was completely separated from the other parts of the image for the frames of the video. Then, the equation of the belt shape curve was obtained using polynomial regression for each frame. Finally, by obtaining the curve of the belt shape, the vibrations of any desired point on the belt became achievable. The results showed that the maximum belt vibration occurred at a point 16 mm apart from the center of the belt with a magnitude of more than 8.5 mm at the engine speed of 4200 rpm. The results also showed that the frequency of the belt vibrations reached 124 Hz. Since the proposed method could provide the instantaneous displacement of all belt points and the equation of the belt curve at any moment, detection of the belt point having the maximum vibration, belt slope, vibration frequency and scatter band of the belt vibration can be obtained as well. According to the results and the capabilities of the proposed method, this machine vision system can reliably be used as a substitute for the traditional method of measuring belt vibrations, i.e. the use of laser displacement sensor.

[DOI: 10.22068/ase.2022.611]

Acknowledgement

We gratefully thank the Irankhodro Powertrain Company (IPCo) for its full support.

References

[1] S. Jafari, M. Kazemi, M. Marzban, S. Moosavian, Health monitoring and performance investigation of accessory belt in an internal combustion engine during critical speeds, The Journal of Engine Research, Vol. 25, (2012), pp. 3-12.

[2] A. Fujii, S. Yonemoto, K. Miyazaki, S. Furumata, K. Okuda, H. Miyazawa, Analysis of the accessory belt lateral vibration in automotive engines, JSAE review, Vol. 23, (2002), pp. 41-47.

[3] P. Castellini, E. Cupido, N. Paone, E.P. Tomasini, Tracking laser doppler vibrometer for linear motion: application to a timing belt, Fourth International Conference on Vibration Measurements by Laser Techniques: Advances and Applications, International Society for Optics and Photonics, (2000), pp. 194-200.

[4] A. Agnani, M. Martarelli, E. Tomasini, V-belt transverse vibration measurement by means of laser Doppler vibrometry, Eighth International Conference on Vibration Measurements by Laser Techniques: Advances and Applications, International Society for Optics and Photonics, (2008), pp. 709819.

[5] H. Chaurasiya, Recent trends of measurement and development of vibration sensors, arXiv preprint arXiv: 1209.5333, (2012).

[6] Y. Hu, S. Zhang, Y. Yan, L. Wang, X. Qian, L. Yang, A smart electrostatic sensor for online condition monitoring of power transmission belts, IEEE Transactions on Industrial Electronics, Vol. 64, (2017), pp. 7313-7322.

[7] M. Ucar, R. Ergun, A. Cengiz, A novel failure diagnosis system design for automotive timing belts, Experimental Techniques, Vol. 38, (2014), pp. 48-53.

[8] Y. Hu, Y. Yan, L. Wang, X. Qian, Non-contact vibration monitoring of power transmission belts through electrostatic sensing, IEEE Sensors Journal, Vol. 16, (2016), pp. 3541-3550.

[9] M. Khazaee, A. Banakar, B. Ghobadian, M.A. Mirsalim, S. Minaei, Remaining useful life (RUL) prediction of internal combustion engine timing belt based on vibration signals and artificial neural network, Neural Computing and Applications, Vol. 33, (2021), pp. 7785–7801.

[10] N. Paul, C. Chung, Application of HDR algorithms to solve direct sunlight problems when autonomous vehicles using machine vision systems are driving into sun, Computers in Industry, Vol. 98, (2018), pp. 192-196.

[11] A.A. Borja, R.M.C. Amongo, D.C. Suministrado, J.P. Pabico, A machine vision assisted mechatronic seed meter for precision planting of corn, 3rd International Conference on Control and Robotics Engineering (ICCRE), IEEE, (2018), pp. 183-187.

[12] D. Bini, D. Pamela, S. Prince, Machine vision and machine learning for intelligent agrobots: A review, 5th International Conference on Devices, Circuits and Systems (ICDCS), IEEE, (2020), pp. 12-16.

[13] A. Martín, R. Lara-Cabrera, F. Fuentes-Hurtado, V. Naranjo, D. Camacho, EvoDeep: a new evolutionary approach for automatic deep neural networks parametrisation, Journal of Parallel and Distributed Computing, Vol. 117, (2018), pp. 180-191.

[14] H. Yaşar, G. Çağıl, O. Torkul, M. Şişci, Cylinder Pressure Prediction of An HCCI Engine Using Deep Learning, Chinese Journal of Mechanical Engineering, Vol. 34, (2021), pp. 1-8.

[15] B. Ramamoorthy, An accurate and robust method for the honing angle evaluation of

[DOI: 10.22068/ase.2022.611]

cylinder liner surface using machine vision, The International Journal of Advanced Manufacturing Technology, Vol. 55, (2011), pp. 611-621.

[16] K.D. Lawrence, R. Shanmugamani, B. Ramamoorthy, Evaluation of image based Abbott–Firestone curve parameters using machine vision for the characterization of cylinder liner surface topography, Measurement, Vol. 55, (2014), pp. 318-334.

[17] F. Xuyun, L. Hui, S. Zhong, L. Lin, Aircraft engine fault detection based on grouped convolutional denoising autoencoders, Chinese Journal of Aeronautics, Vol. 32, (2019), pp. 296-307.

[18] S. Capela, R. Silva, S.R. Khanal, A.T. Campaniço, J. Barroso, V. Filipe, Engine Labels Detection for Vehicle Quality Verification in the Assembly Line: A Machine Vision Approach, Portuguese Conference on Automatic Control, Springer, (2020), pp. 740-751.

[19] J. Rochussen, P. Kirchen, Robust image segmentation for feature extraction from internal combustion engine in-cylinder images, Measurement Science and Technology, Vol. 32 (2020), pp. 015302.

[20] PSA flapping test procedure, No. DTI/DPMO/AMMT/MVAM, (2002).

[21] A. Voulodimos, N. Doulamis, A. Doulamis, E. Protopapadakis, Deep learning for computer vision: A brief review, Computational intelligence and neuroscience, (2018).

[22] Y. LeCun, Y. Bengio, G. Hinton, Deep learning, Nature, Vol. 521, (2015), pp. 436-444.

[23] R. Girshick, J. Donahue, T. Darrell, J. Malik, Rich feature hierarchies for accurate object detection and semantic segmentation, Proceedings of the IEEE conference on computer vision and pattern recognition, (2014), pp. 580-587.

[24] R. Girshick, Fast r-cnn, Proceedings of the IEEE international conference on computer vision, (2015), pp. 1440-1448.

[25] S. Ren, K. He, R. Girshick, J. Sun, Faster r-cnn: Towards real-time object detection with region proposal networks, Advances in neural information processing systems, Vol. 28, (2015), pp. 91-99.

[26] C. Nuzzi, S. Pasinetti, M. Lancini, F. Docchio, G. Sansoni, Deep learning based machine vision: first steps towards a hand gesture recognition set up for collaborative robots, Workshop on Metrology for Industry 4.0 and IoT, IEEE, (2018), pp. 28-33.

[27] K. He, G. Gkioxari, P. Dollár, R. Girshick, Mask r-cnn, Proceedings of the IEEE international conference on computer vision, (2017), pp. 2961-2969.

[28] E. Ostertagová, Modelling using polynomial regression, Procedia Engineering, Vol. 48, (2012), pp. 500-506.

[29] Y.W. Chang, C.J. Hsieh, K.W. Chang, M. Ringgaard, C.J. Lin, Training and testing low-degree polynomial data mappings via linear SVM, Journal of Machine Learning Research, Vol. 11, (2010), pp. 1471−1490.

[DOI: 10.22068/ase.2022.611]